minerals

Supplementary materials: The Evaluation of Clay Suitability for Geopolymer Technology

Tomáš Hanzlíček, Ivana Perná, Kateřina Uličná, Václav Římal and Helena Štěpánková

A. Geopolymer solids

Figure S1. Geopolymer solid prepared from metakaolin Kadan.

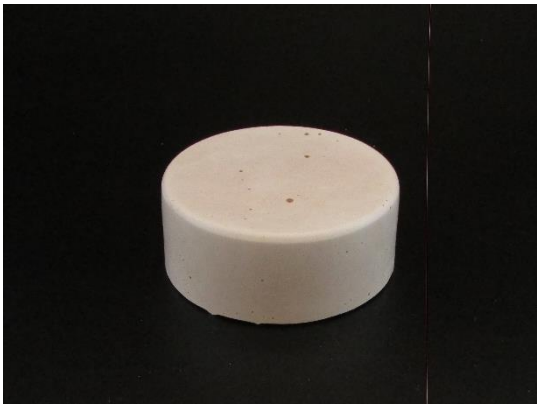

Figure S2. Geopolymer solid prepared from metakaolin Ledce.

Figure S3. Geopolymer solid prepared from metakaolin Sedlec.

Figure S4. Geopolymer solid prepared from metakaolin Strelec.

Figure S5. Geopolymer solid prepared from metakaolin Vidnava.

Figure S6. Geopolymer solid prepared from metakaolin Kaznejov.

Figure S7. Geopolymer solid prepared from metakaolin Provodin.

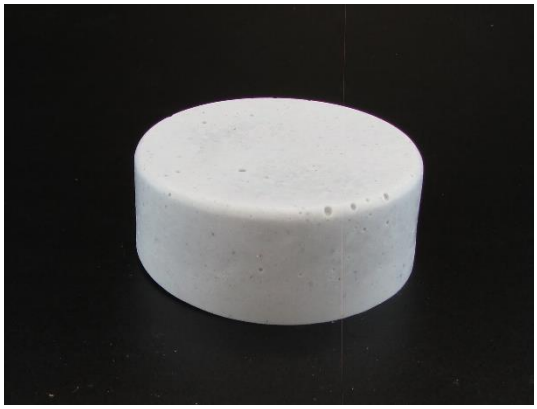

Figure S8. Geopolymer solid prepared from metakaolin Sri Lanka.

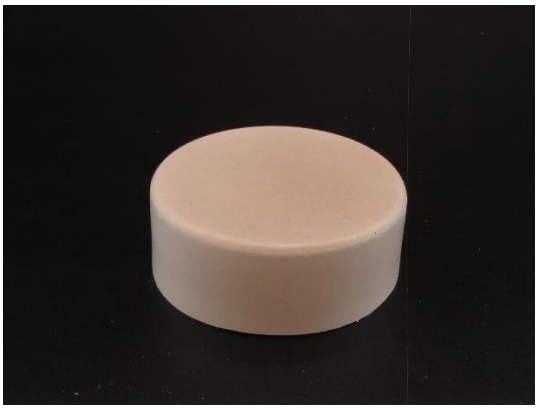

Figure S9. Geopolymer solid prepared from metakaolin Ukraine.

Figure S10. Geopolymer solid prepared from metakaolin Brazil "B".

Figure S11. Geopolymer solid prepared from metakaolin Brazil "R".

A. Infrared analysis

The Fourier transform infrared (FTIR) spectra were measured using a iS50 (Thermo Nicolet Instruments Co., Madison, USA) spectrometer by the attenuated total reflection (ATR) using diamond crystal, averaging 64 scans with resolution 4 cm^{-1} in the range of 4000–400 cm^{-1}. Processing of obtained spectra were performed using the OMNIC Software 2019.

Figure S12–S22 demonstrate a comparison of the spectra of original metakaolins and corresponding geopolymers in the „fingerprint" region (1300 – 400 cm^{-1}). The spectral differences are visible in the low-wavenumber region between 800 and 400 cm^{-1} and the middle-wavenumber region between 1250 and 800 cm^{-1}. In the low-wavenumber region, the spectrum of metakaolin had characteristic bands at ~470 cm^{-1} and ~800 cm^{-1} assigned to tetrahedral bending mode of T-O (T = Si or Al) and bending mode of Si-O-Al, respectively. However, in cases of samples Provodin and Strelec (Figs. S21 and S22), this band is overlapped by double band belonged to quartz. After geopolymerization, both intensities of these two bands decreased and the new band appeared at ~700 cm^{-1} (spectrum of geopolymers) indicating the formation of tetrahedral Al [Al-O4] [1].

In the middle-wavenumber region, the positions of the strong asymmetrical stretching vibration bands of the Si-O bond in metakaolin, located in the range 1054 - 1082 cm^{-1} (dark blue spectra), have been found to shift to lower wavenumbers (992 - 1002 cm^{-1}) in the spectra of geopolymers (red spectra). This shift proves the formation of geopolymer bonds. After geopolymerization, the chemical environment around regular arranged chain structures of the Si-O bond altered, along with the formation of Al-O-Si bonds [2].

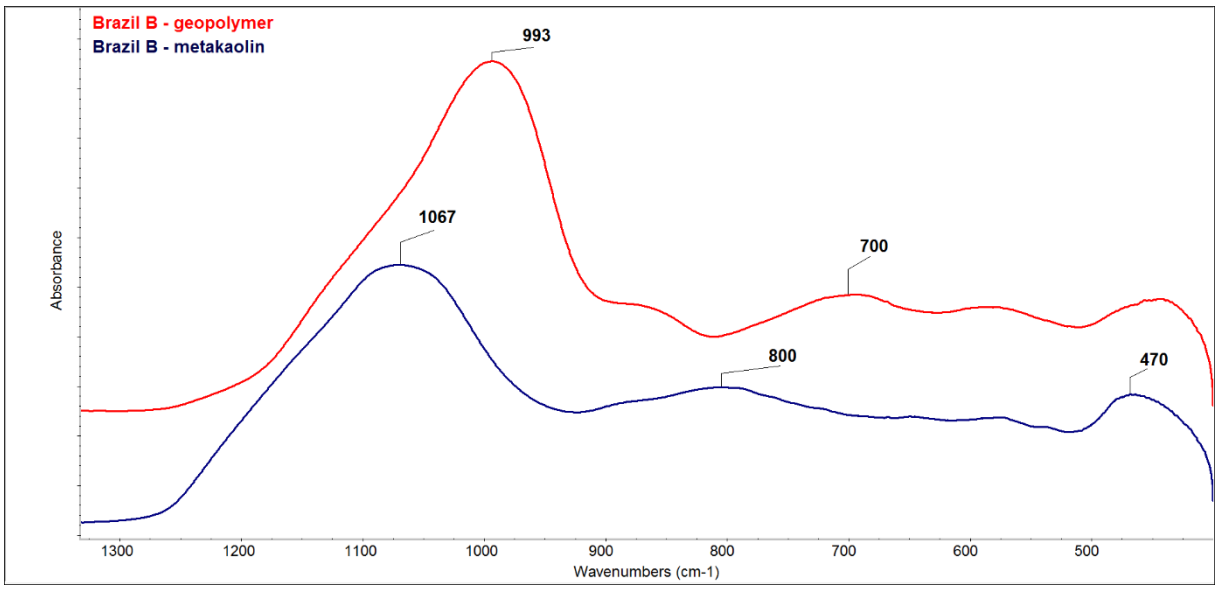

Figure S12. Comparison of infrared spectra of metakaolin Brazil "B"with corresponding geopolymer matrix.

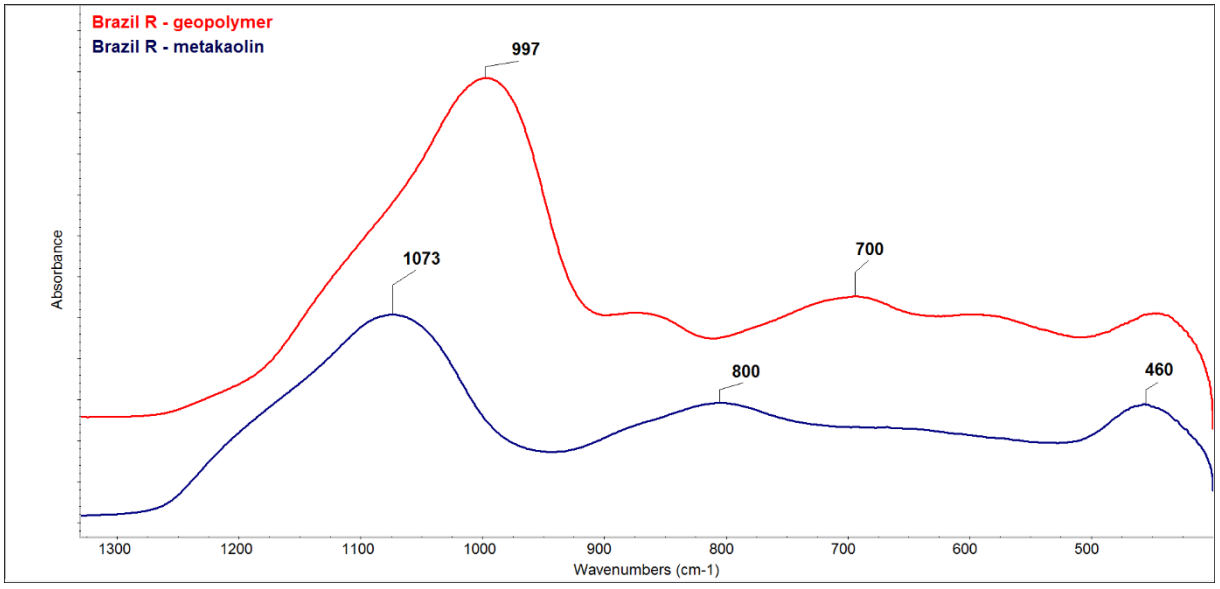

Figure S13. Comparison of infrared spectra of metakaolin Brazil "R"with corresponding geopolymer matrix.

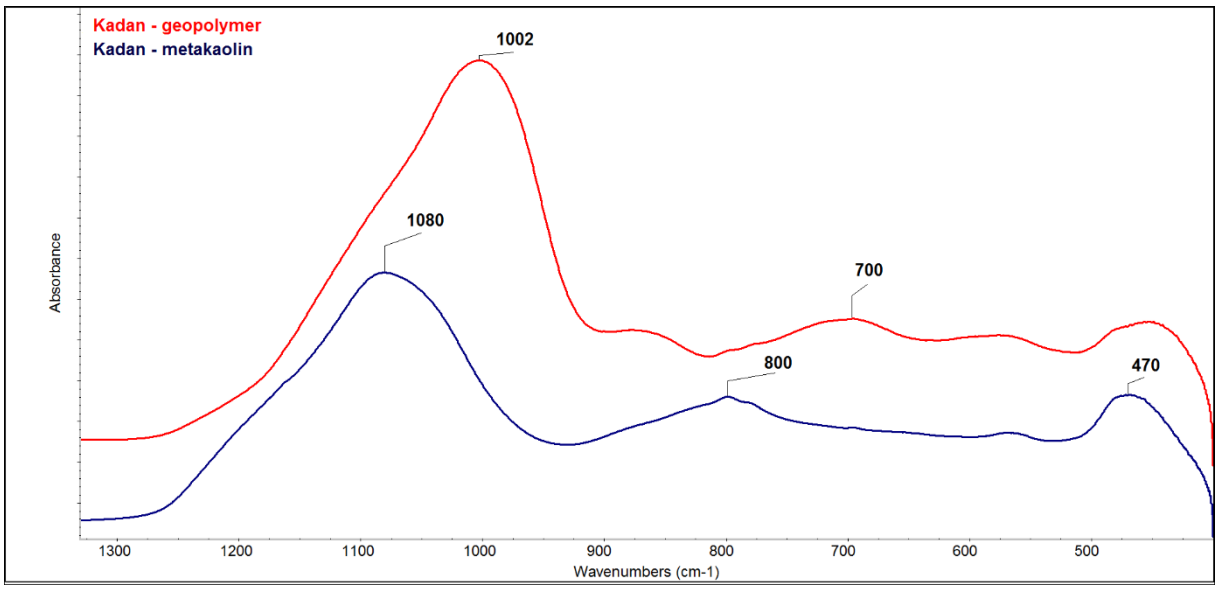

Figure S14. Comparison of infrared spectra of metakaolin Kadan with corresponding geopolymer matrix.

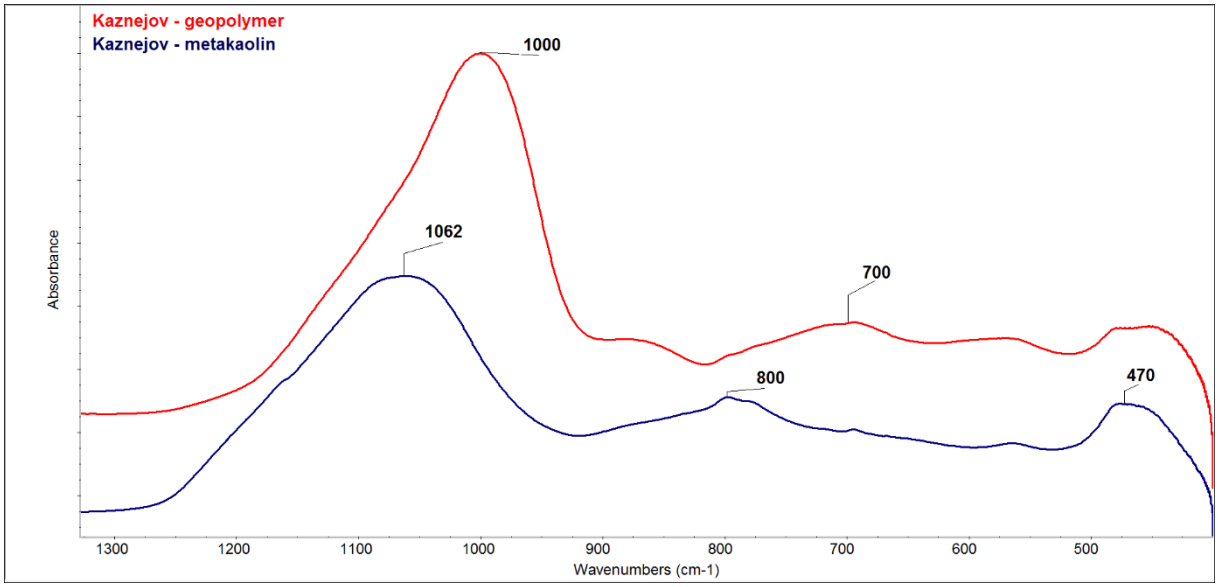

Figure S15. Comparison of infrared spectra of metakaolin Kaznejov with corresponding geopolymer matrix.

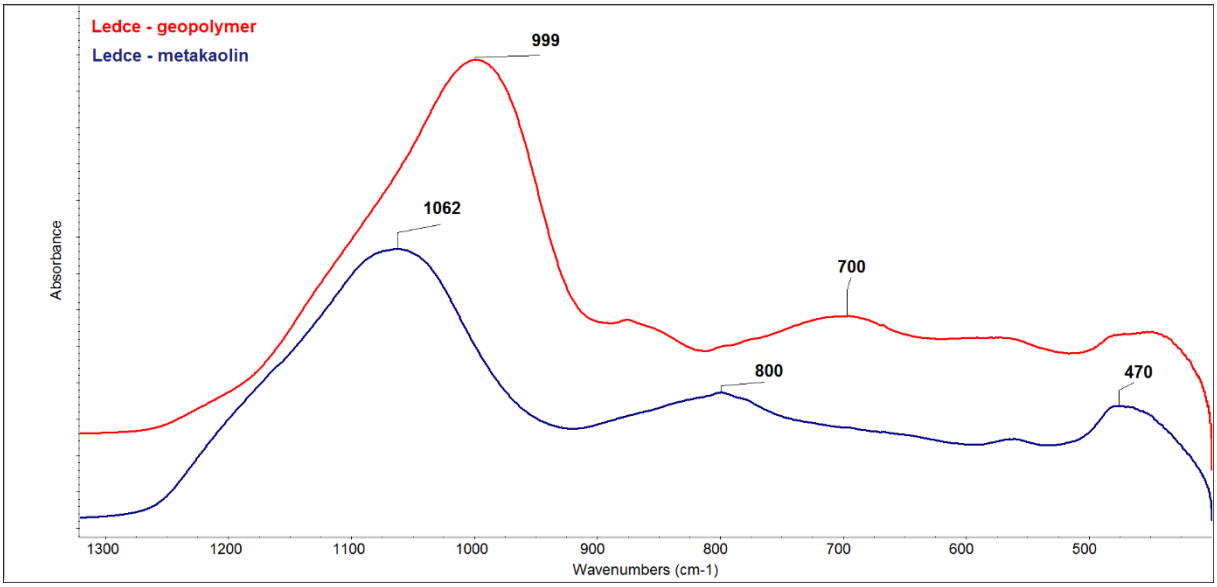

Figure S16. Comparison of infrared spectra of metakaolin Ledce with corresponding geopolymer matrix.

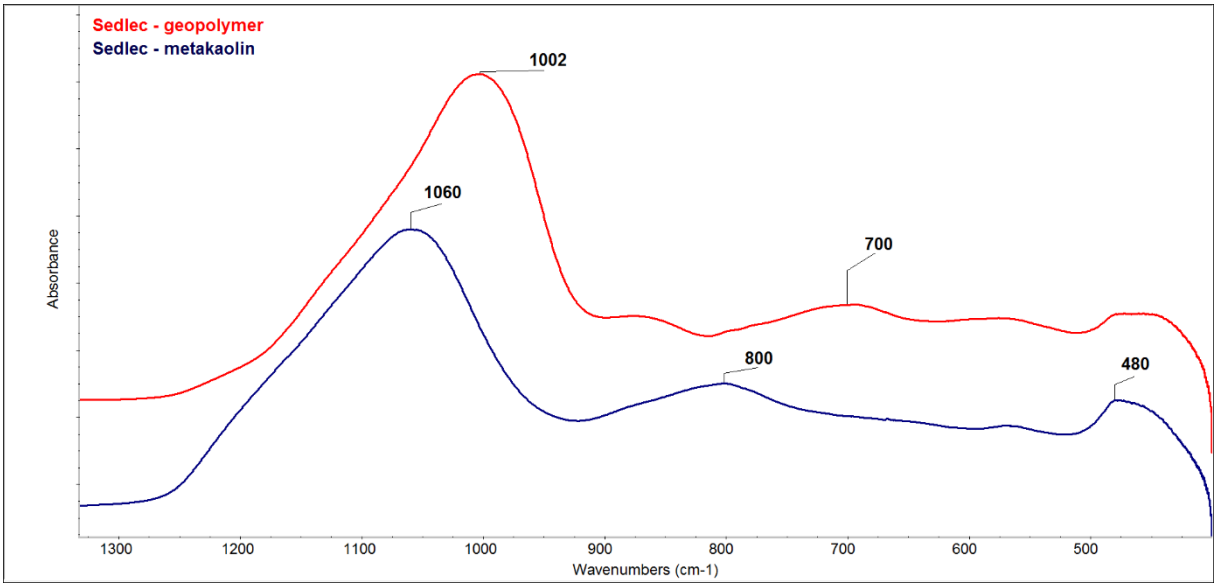

Figure S17. Comparison of infrared spectra of metakaolin Sedlec with corresponding geopolymer matrix.

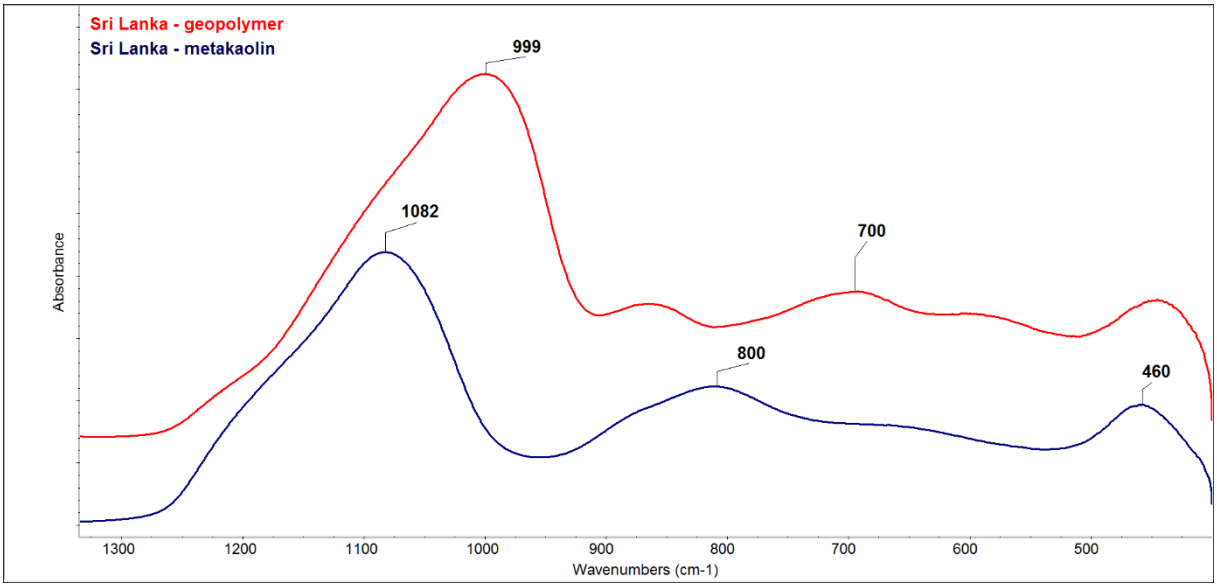

Figure S18. Comparison of infrared spectra of metakaolin Sri Lanka with corresponding geopolymer matrix.

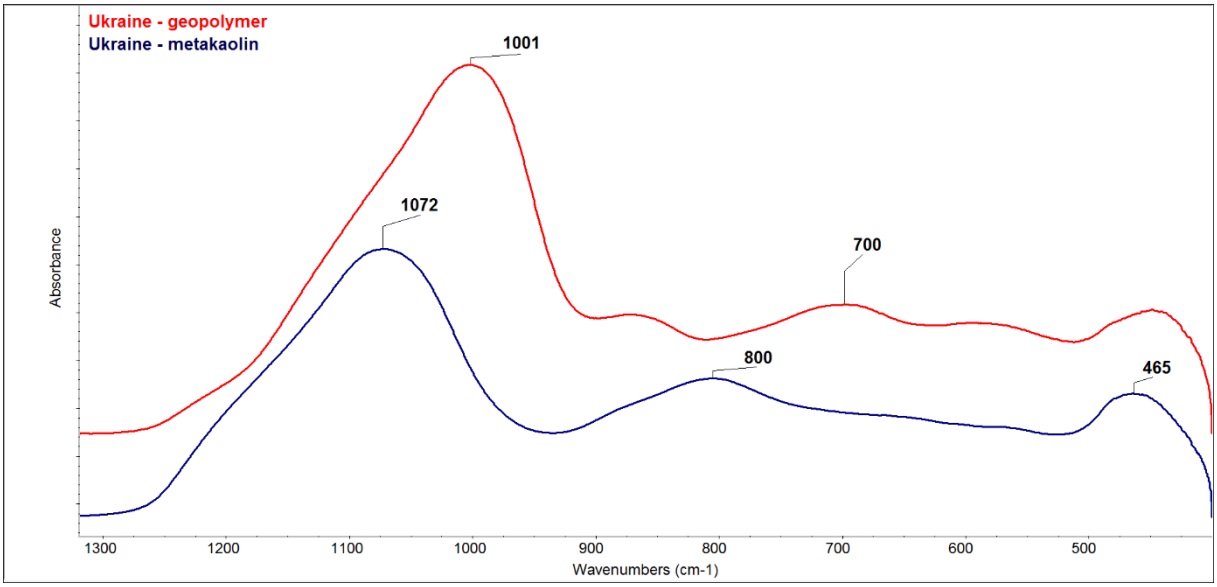

Figure S19. Comparison of infrared spectra of metakaolin Ukraine with corresponding geopolymer matrix.

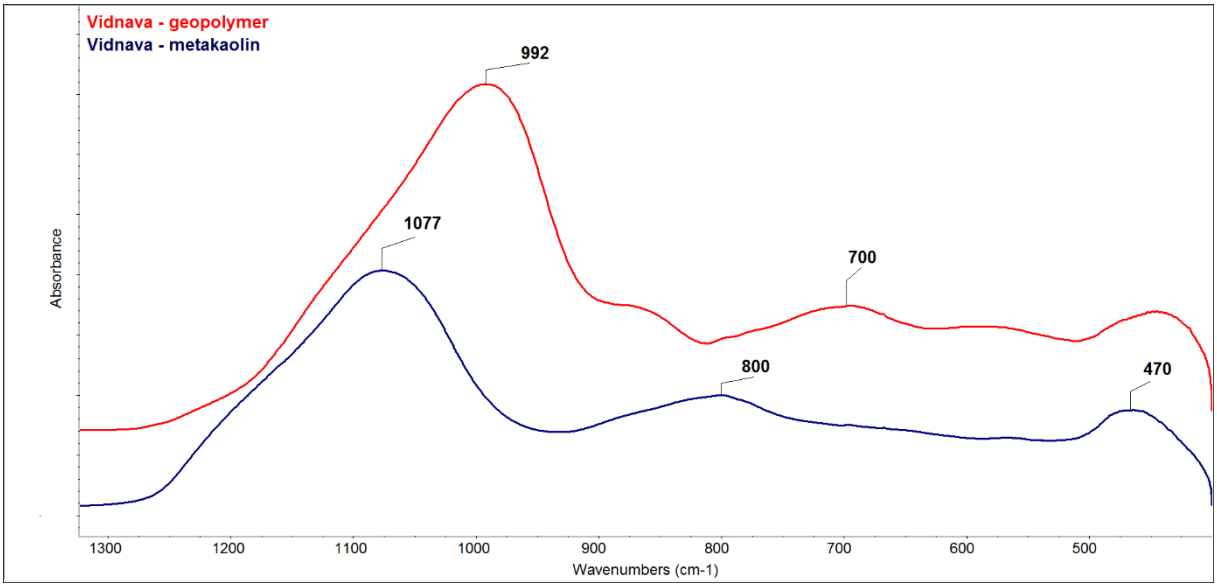

Figure S20. Comparison of infrared spectra of metakaolin Vidnava with corresponding geopolymer matrix.

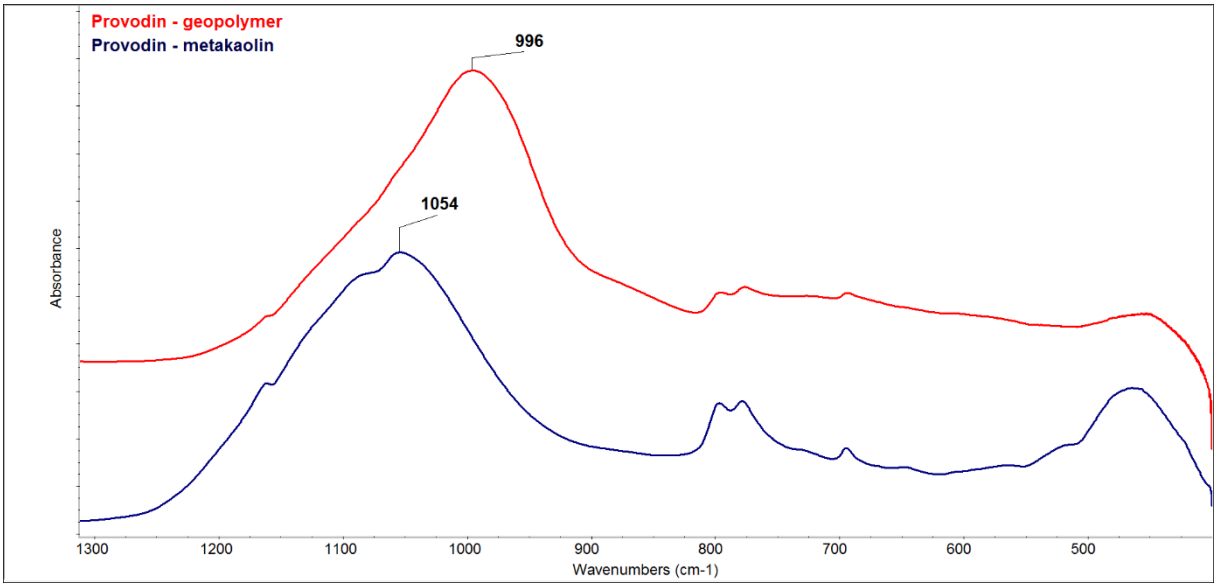

Figure S21. Comparison of infrared spectra of metakaolin Provodin with corresponding geopolymer matrix.

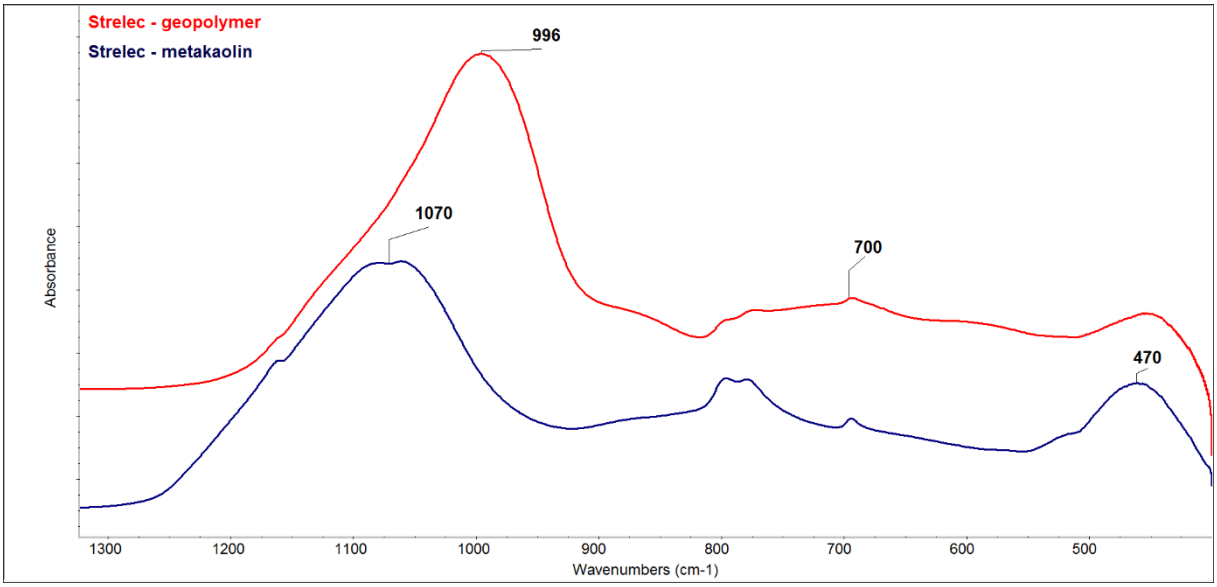

Figure S22. Comparison of infrared spectra of metakaolin Strelec with corresponding geopolymer matrix.

1. López, F.J., Sugita, S., Tagaya, M., Kobayashi, T. Metakaolin-based geopolymers for targeted adsorbents to heavy metal ion separation. J. Mater. Sci. Eng **2014,** 2, 16–27, doi:10.4236/msce.2014.27002.
2. Tippayasam, C., Balyore, P., Thavorniti, P., Kamseu, E., Leonelli, C., Chindaprasirt, P., Chaysuwan, D. Potassium alkali concentration and heat treatment affected metakaolin-based geopolymer. Constr. Build. Mater. **2016**, 104, 293–297, doi:10.1016/j.conbuildmat.2015.11.027.

A. XRD patterns

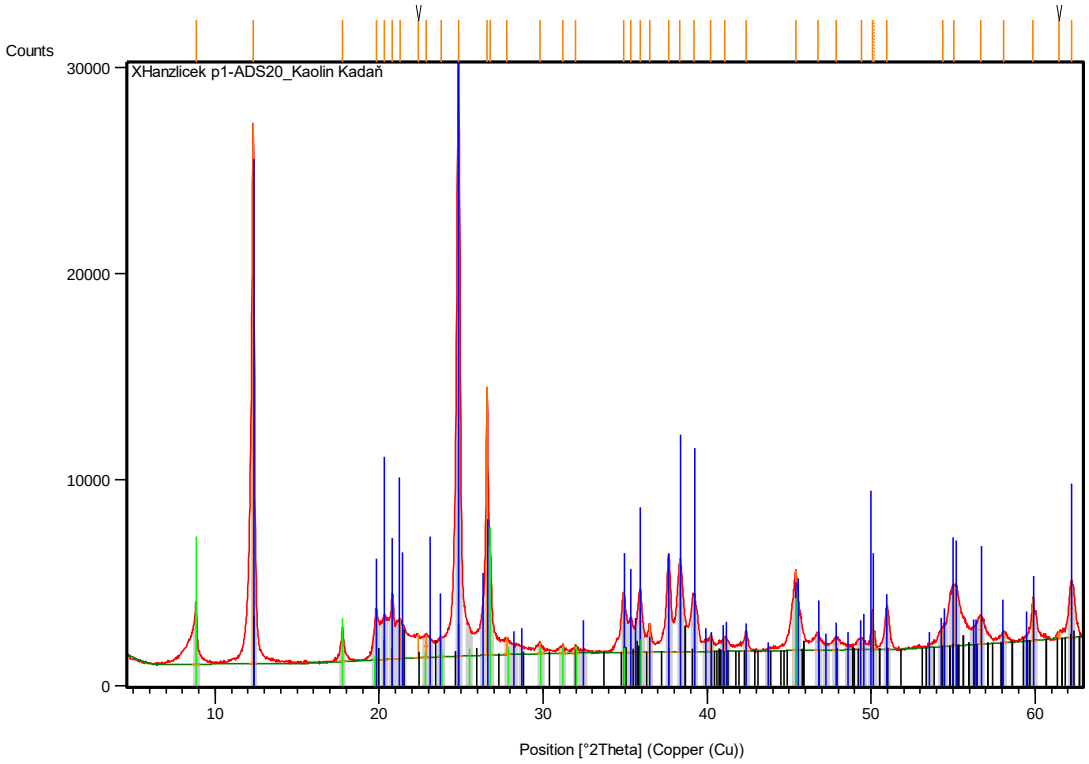

Figure S23. XRD pattern of kaolin Kadan.

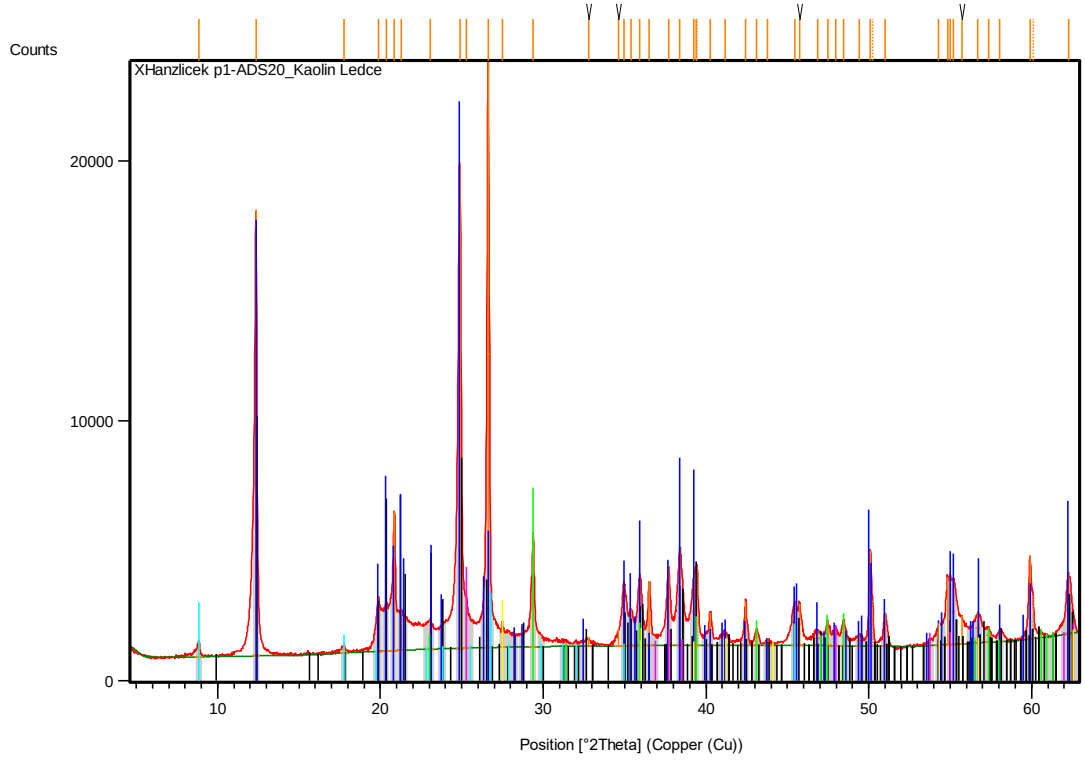

Figure S24. XRD pattern of kaolin Ledce.

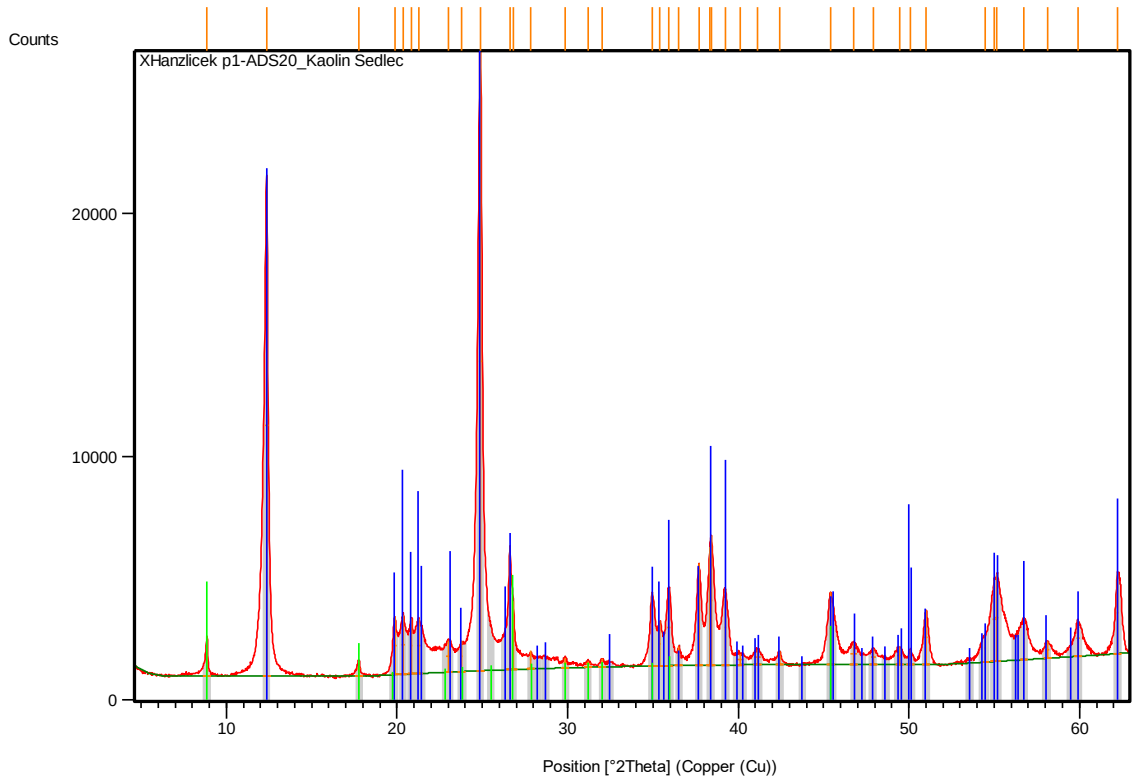

Figure S25. XRD pattern of kaolin Sedlec.

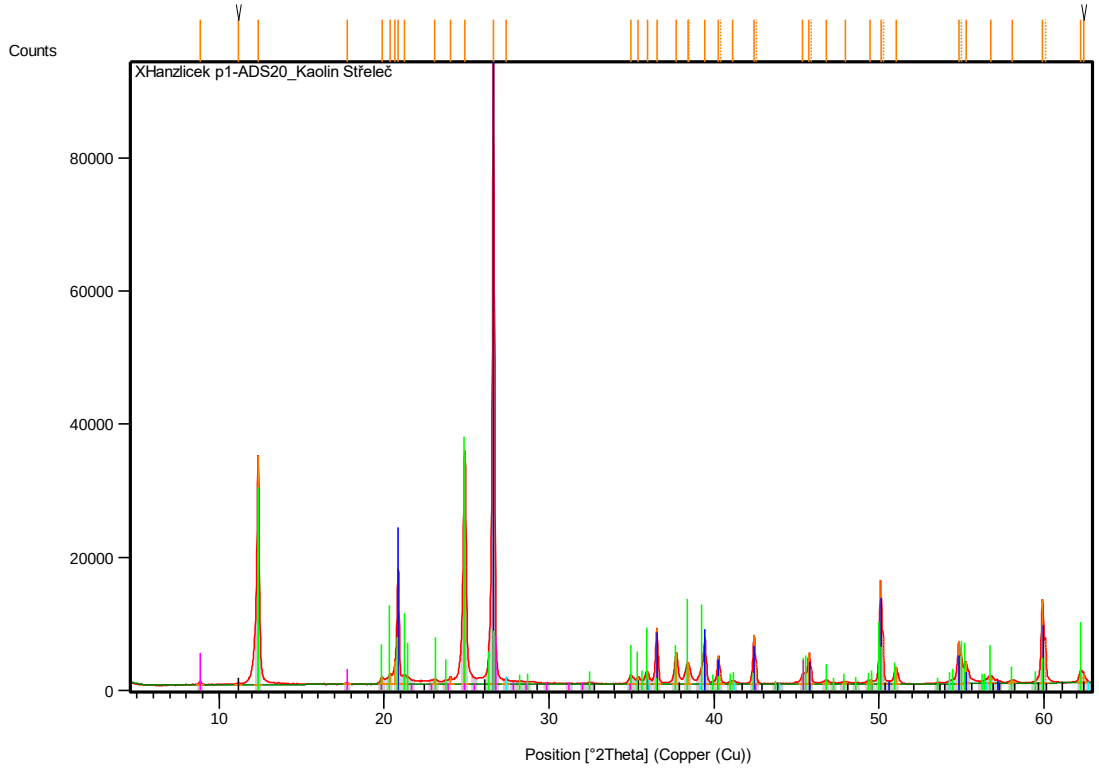

Figure S26. XRD pattern of kaolin Strelec.

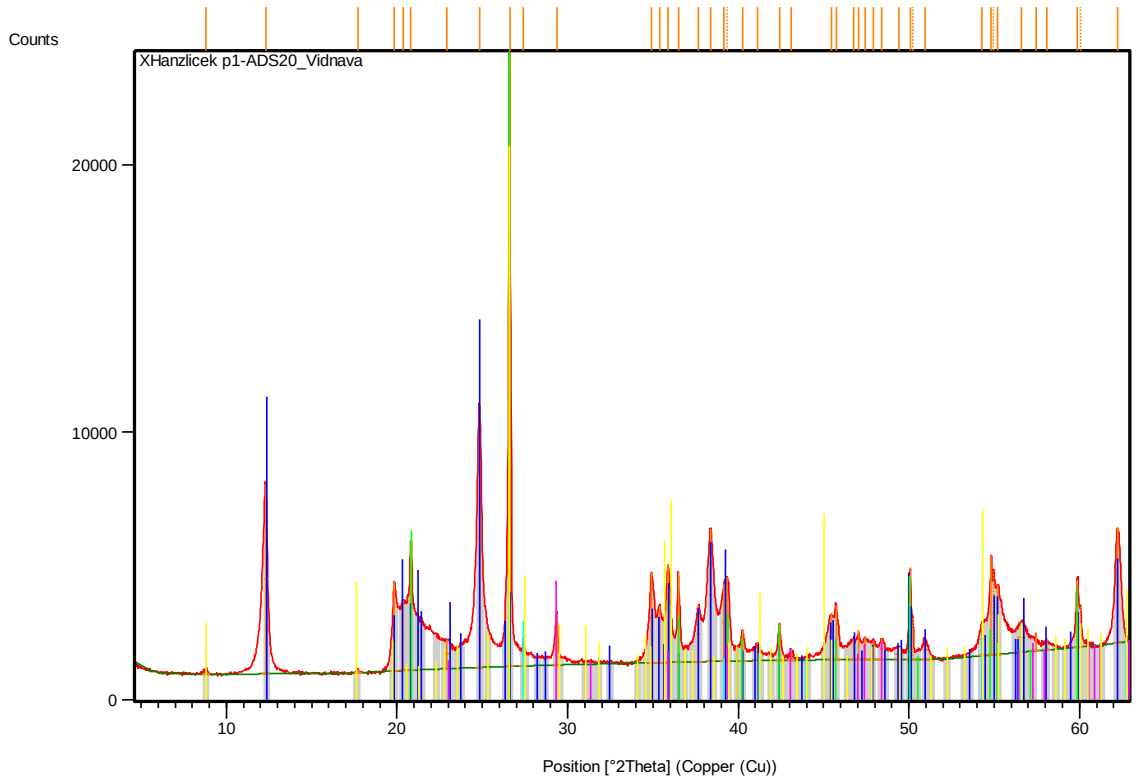

Figure S27. XRD pattern of kaolin Vidnava.

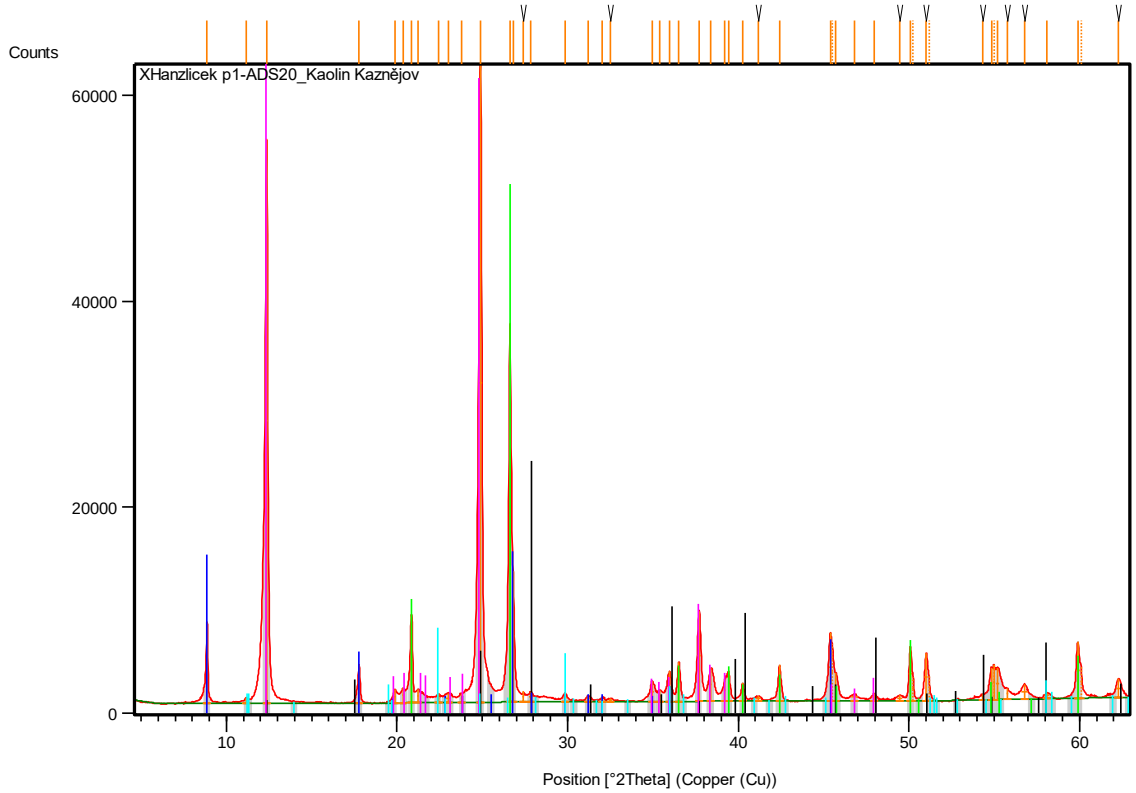

Figure S28. XRD pattern of kaolin Kaznejov.

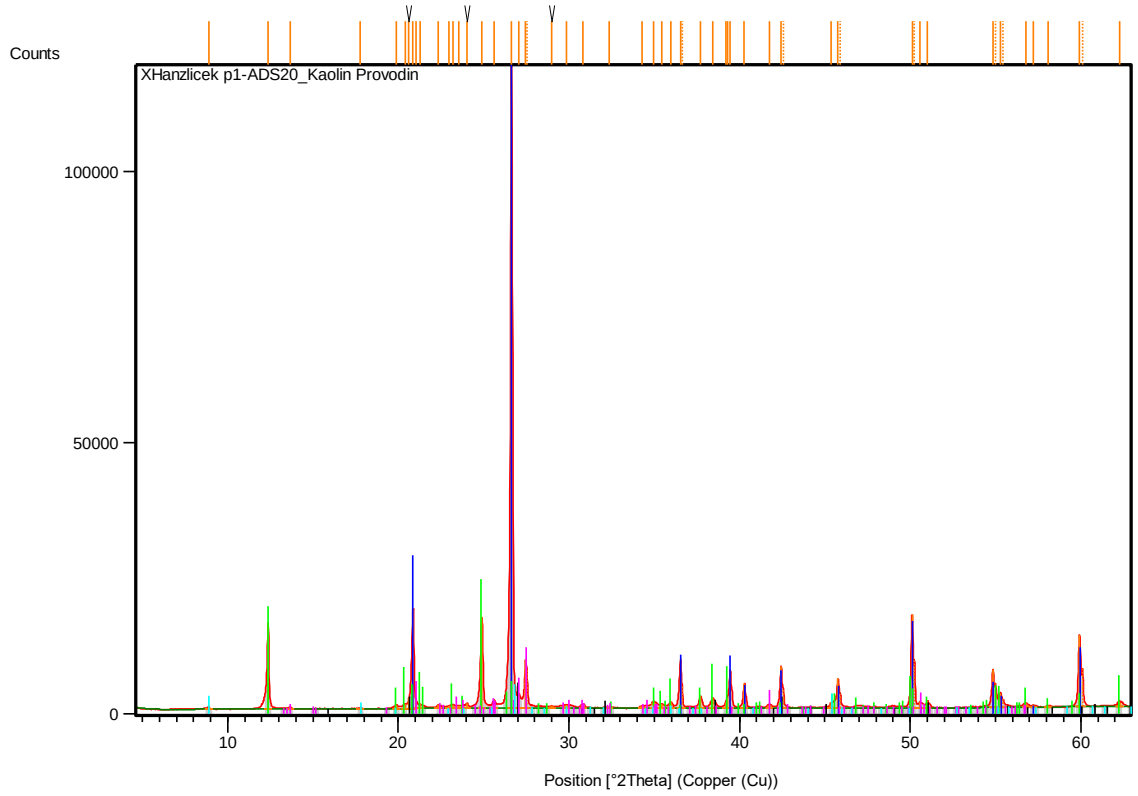

Figure S29. XRD pattern of kaolin Provodin.

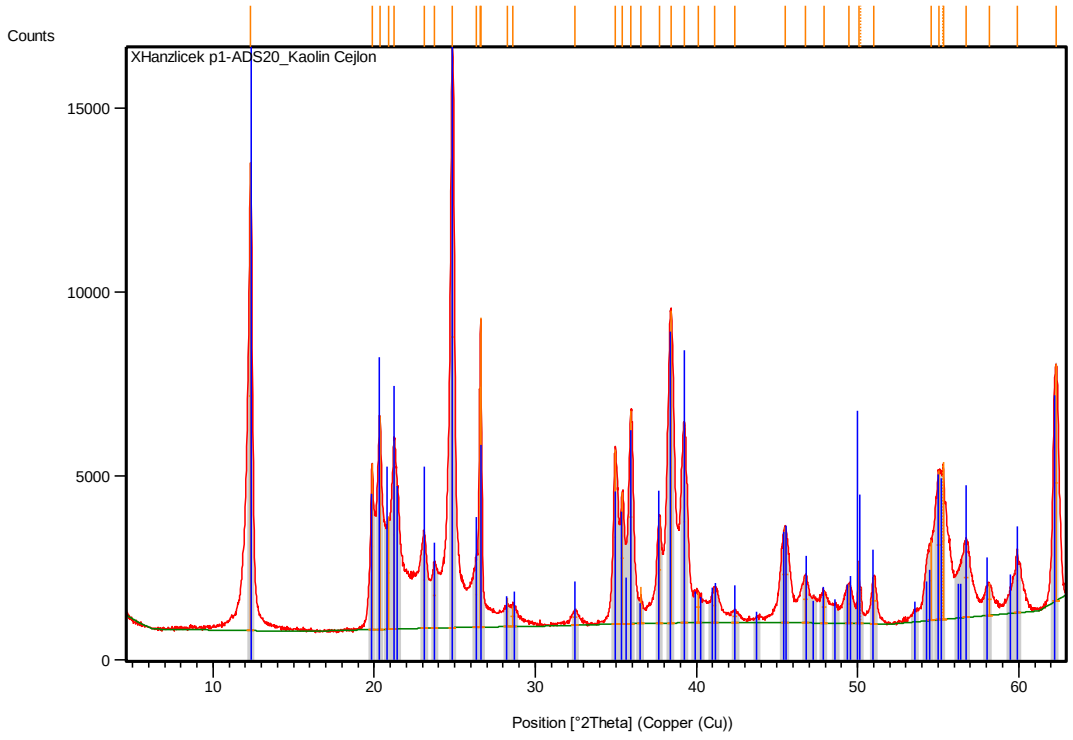

Figure S30. XRD pattern of kaolin Sri Lanka.

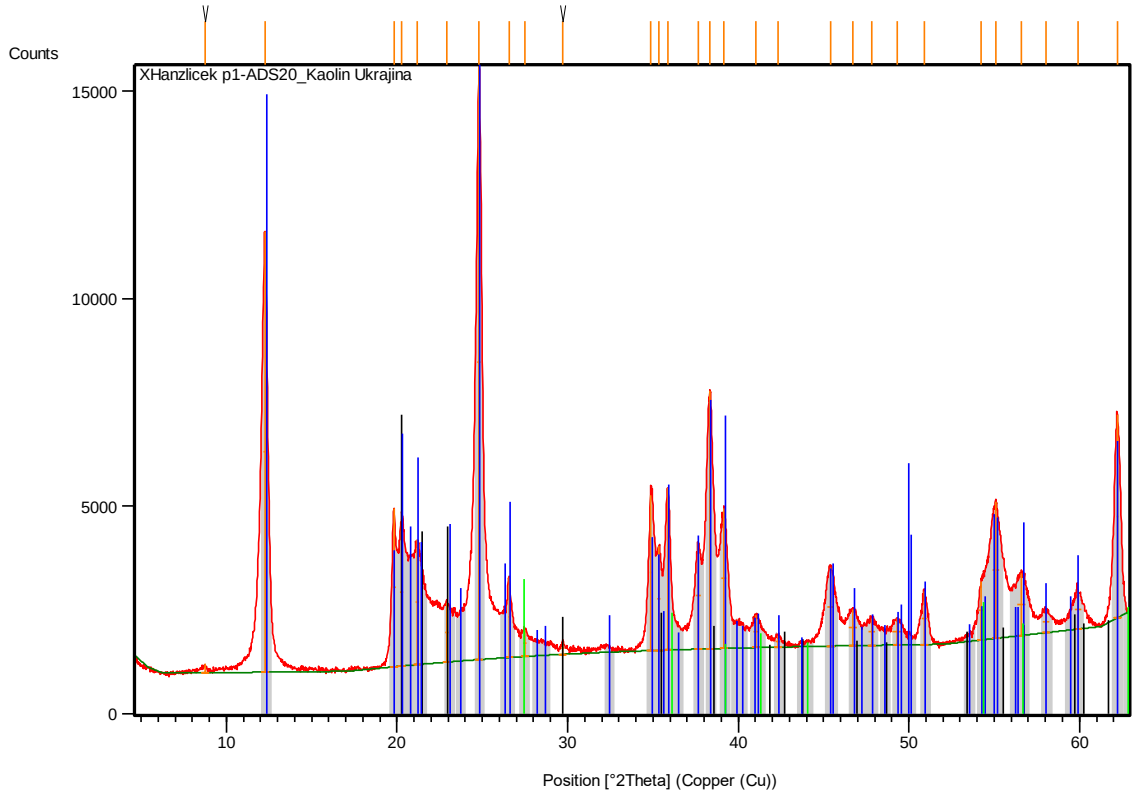

Figure S31. XRD pattern of kaolin Ukraine.

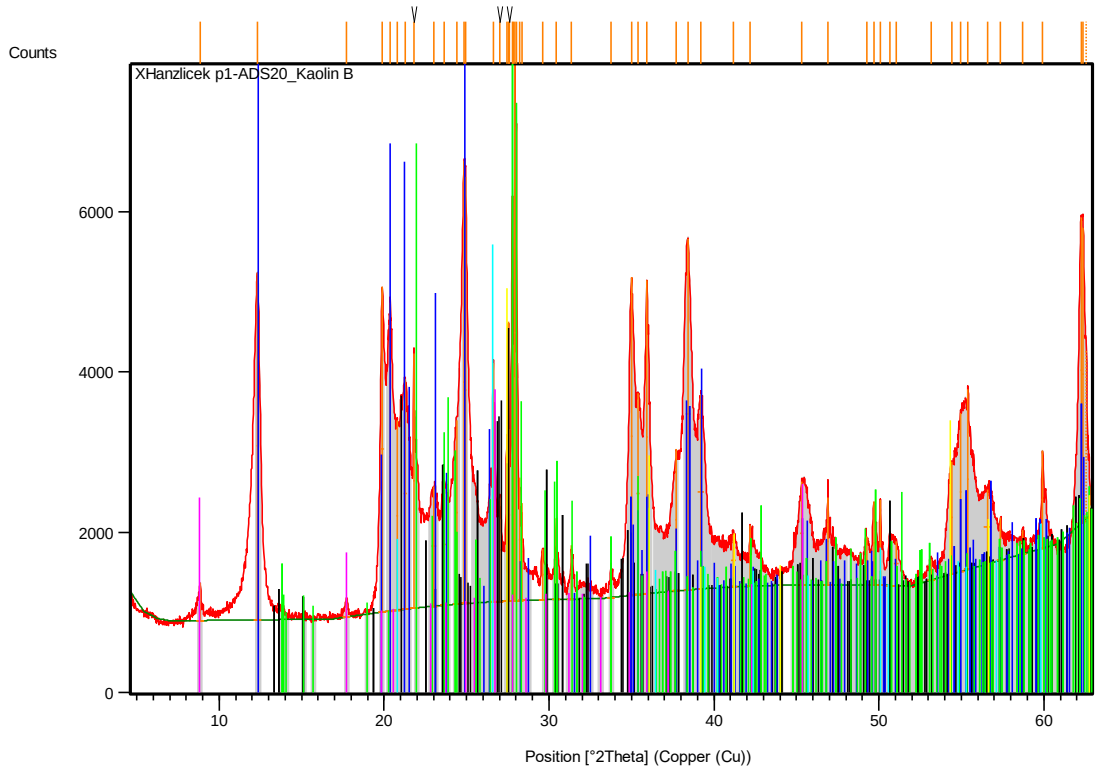

Figure S32. XRD pattern of kaolin Brazil "B".

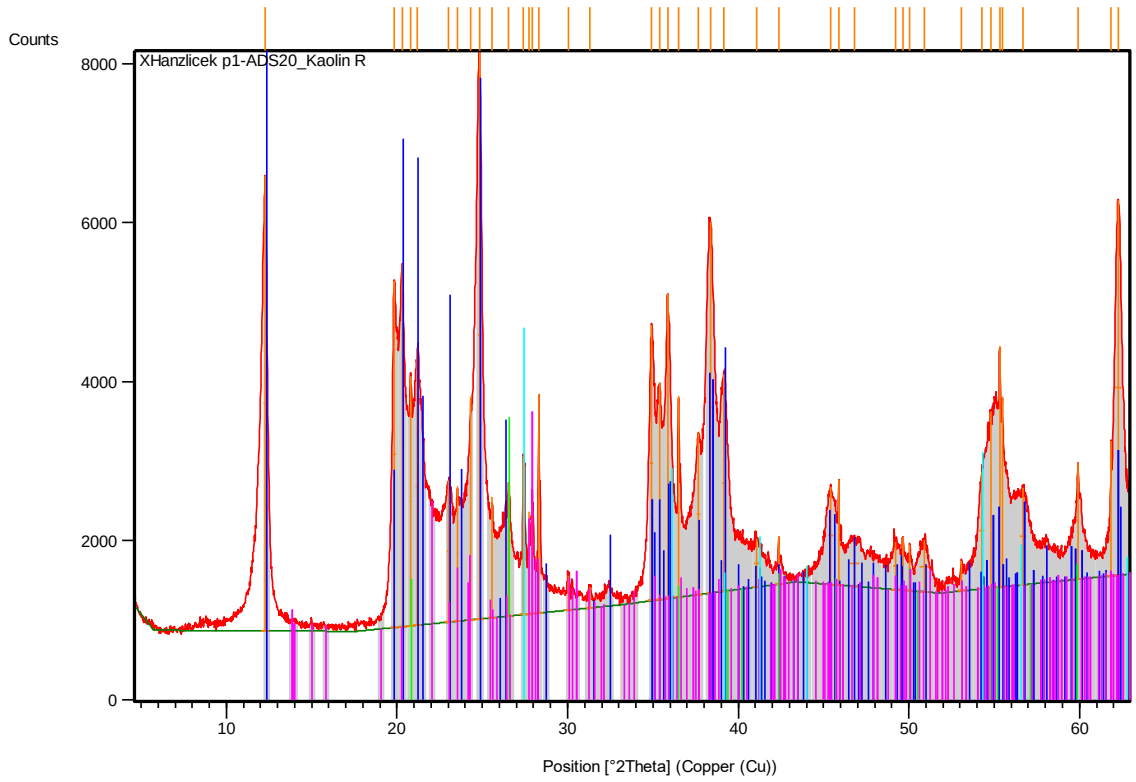

Figure S33. XRD pattern of kaolin Brazil "R".